

Supporting information

Bioengineering of a human innervated cardiac muscle model

Lennart Valentin Schneider^{1,2,5}, Bao Guobin^{1,2}, Aditi Methi⁴, Ole Jensen³, Kea Aline Schmoll^{1,5}, Michael Gani Setya¹, Sadman Sakib⁴, Aminath Luveysa Fahud¹, Jürgen Brockmüller³, André Fischer^{4,5}, Norman Y. Liaw^{1,2}, Wolfram-Hubertus Zimmermann^{1,2,4,5,6}, Maria-Patapia Zafeiriou^{1,2,5*}

¹Institute of Pharmacology and Toxicology, University Medical Center, Georg-August-University, Göttingen, Germany

²DZHK (German Center for Cardiovascular Research), partner site Göttingen, Germany

³Department of Clinical Pharmacology, University Medical Center, Georg-August-University, Göttingen, Germany

⁴German Center for Neurodegenerative Diseases, Göttingen, Germany

⁵MBExC (Multi-Scale Bioimaging Excellence Cluster), Göttingen, Germany

⁶Fraunhofer Institute for Translational Medicine and Pharmacology (ITMP), Göttingen, Germany

Table of content

Supplementary Figure

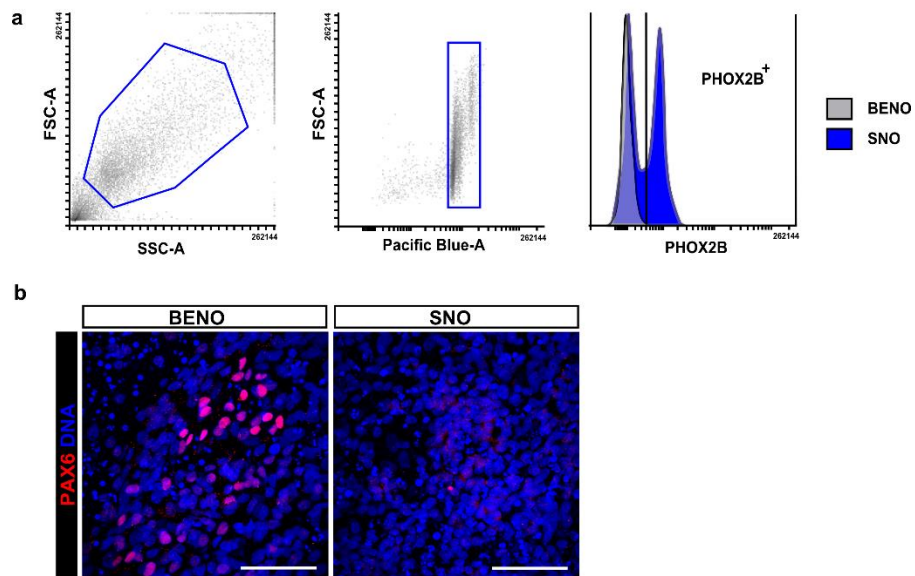
- **Supplementary Figure 1**| Sympathetic neural progenitor analysis in d15 SNO
- **Supplementary Figure 2**| Sympathetic neuron immunofluorescence analysis in d30 SNO
- **Supplementary Figure 3**| Identification of non-SN cells co-developing in SNO
- **Supplementary Figure 4**| Neurotransmitter quantification by LC-MS/MS analysis
- **Supplementary Figure 5**| Effect of nicotinic acid on electrical activity of SNO d73-87
- **Supplementary Figure 6**| Reproducibility of SNO differentiation protocol in three iPSC-lines
- **Supplementary Figure 7**| Gating strategy for sorting nuclei from frozen iEHM lysates using 7AAD staining
- **Supplementary Figure 8**| Cell cluster annotation of snRNA-sequencing
- **Supplementary Figure 9**| Expression analysis of ion channels across the cell types from snRNA-sequencing
- **Supplementary Figure 10**| Analysis of cardiomyocyte and fibroblast subcluster in the iEHM
- **Supplementary Figure 11**| Investigation of neuro-cardiac junctions in iEHM
- **Supplementary Figure 12**| Vascular network development in SNO, EHM and iEHM
- **Supplementary Figure 13**| Identification of pacemaker-like cells in iEHM
- **Supplementary Figure 14**| Details of pharmacological stimulation of iEHM

Supplementary Materials

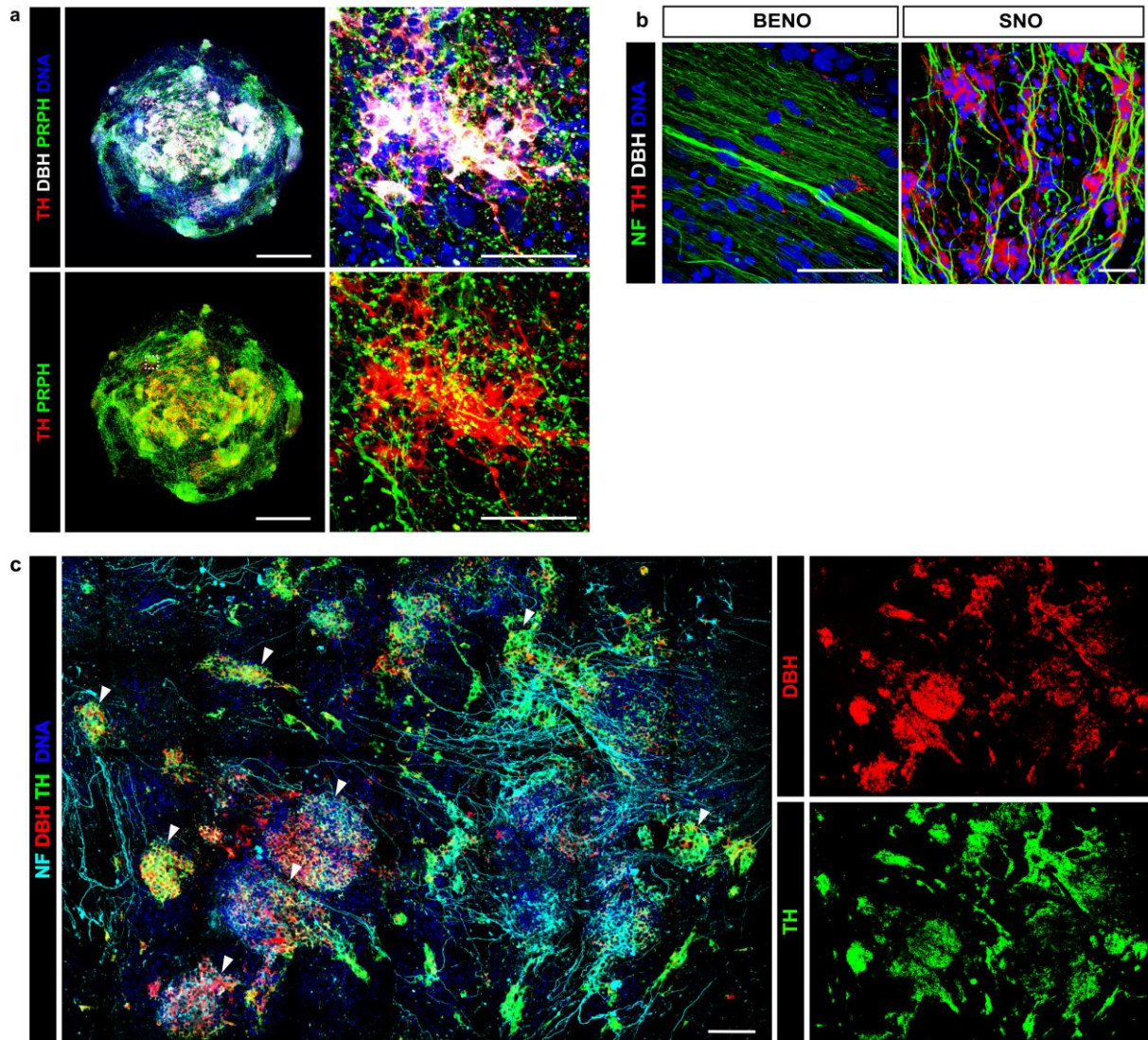
- **Supplementary Table 1**| Detection parameters for a second compound-specific mass transition used as qualifier
- **Supplementary Table 2**| List of primer for quantitative real-time PCR
- **Supplementary Table 3**| List of primary and secondary antibodies

List of Supplementary Videos

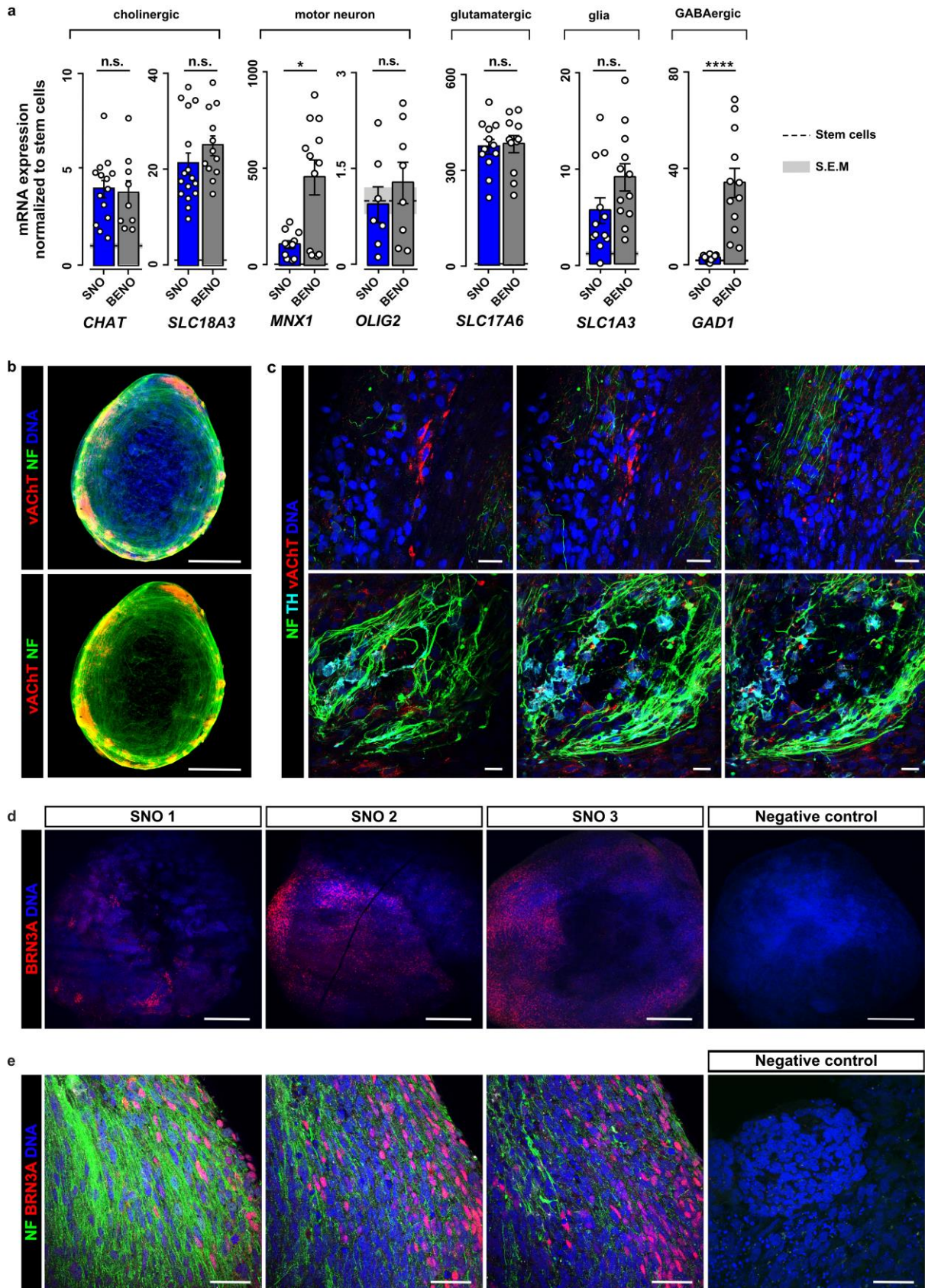
Supplementary Figures



Supplementary Figure 1| Sympathetic neural progenitor analysis in d15 SNO. **a**, Gating of flow cytometry analysis of d15 neural progenitor cells isolated from SNO and BENO stained for DNA and PHOX2B. SSC-A=side scatter-area, FSC-A=forward scatter-area. **b**, Immunofluorescence of d15 SNO and BENO stained by cortical marker PAX6 (red). Scale bar, 50 μ m.

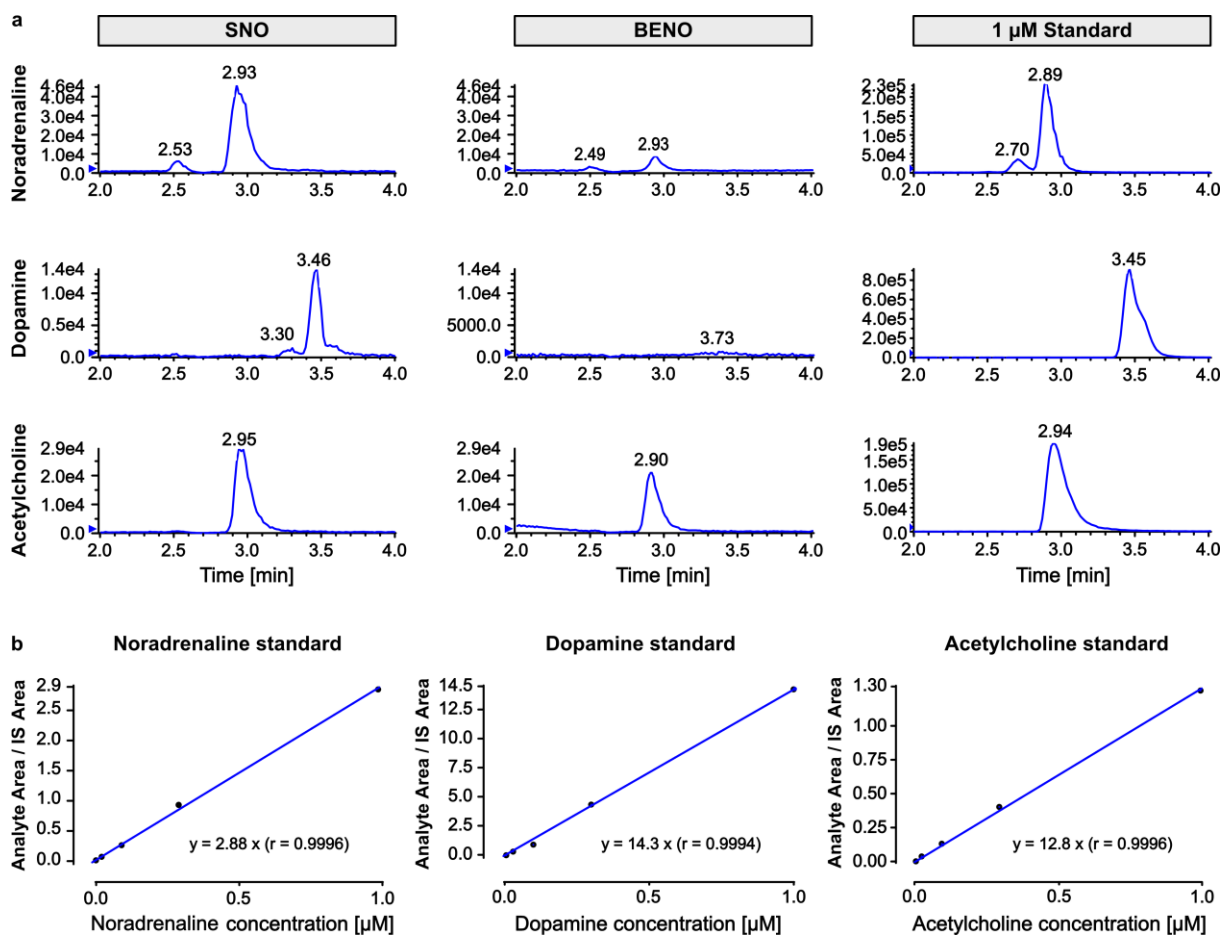


Supplementary Figure 2| Sympathetic neuron immunofluorescence analysis in d30 SNO. *a*, Representative image of d41 SNO stained for sympathetic marker TH (red), DBH (greys), peripheral neuron marker PRPH (green), and DNA (blue). Scale bar, 500 μm . **(Right)** Close-up view. Scale bar, 50 μm . *b*, Close-up view shows sympathetic neurons co-stained by DBH (red), NF (green) and DNA (blue) in SNO showing ganglia-like structures **(Right)**. BENO did not contain sympathetic neurons **(Left)**. Scale bars, 50 μm . *c*, High resolution imaging of SNO stained for sympathetic marker TH (red) and DBH (grey) as well as NF (green) and DNA (blue) showing widespread sympathetic ganglia-like structures (marked by white arrowheads). Scale bar, 100 μm .

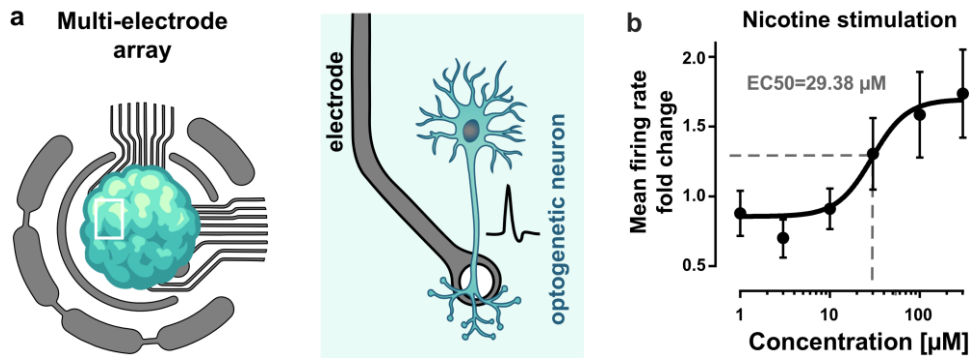


Supplementary Figure 3 | Identification of non-SN cells co-developing in SNO. a, Expression analysis of cholinergic marker (CHAT, SLC18A3 [aka VACHT]), GABAergic (GAD1), motor (MNX1, OLIG2), glutamatergic (SLC17A6 [aka VGLUT2]) neuron marker and astrocyte (SLC1A3 [aka GLAST]) marker for SNO and BENO at d41 normalized to GAPDH expression. SNO and BENO were normalized to expression in undifferentiated stem cells. Mann-Whitney test or Student's t-test were performed, depending on normality

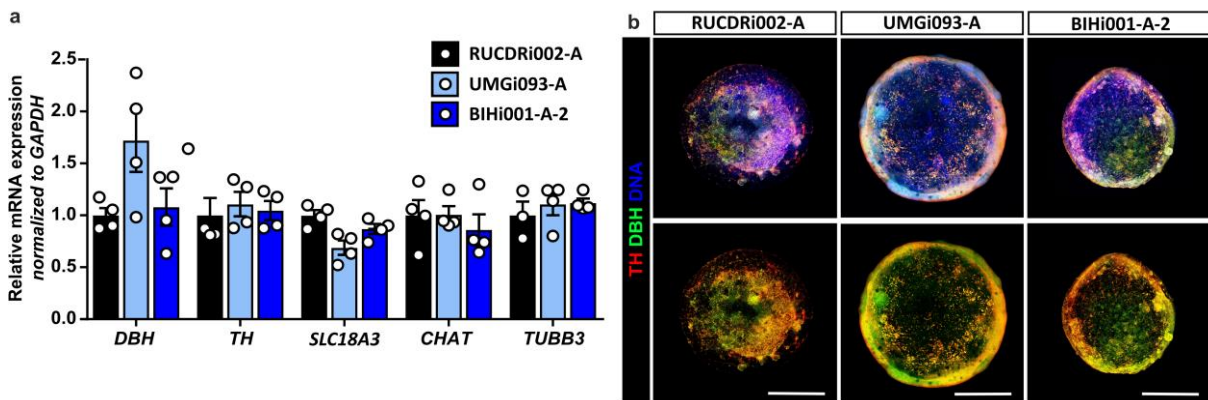
of the data set. 3-4 independent differentiations, 3-4 biological replicates per differentiation ($n=9-16$) $p \leq 0.05$, $p^{***} \leq 0.001$, $p^{****} \leq 0.0001$. **b**, WhIF of d30 SNO stained for cholinergic marker vAChT (red), NF (green) and DNA (blue). Scale bar, 500 μm . **c**, Close-up view of cholinergic neurons vAChT (red) and sympathetic neurons marked by TH (cyan) from two different SNO regions. Scale bar, 20 μm . **d**, IF-staining of three individual SNO at d41 for sensory neuron marker BRN3A (red) and nuclear counterstaining (blue). (**Far right**) d41 SNO as no primary antibody control. Scale bar, 200 μm . **e**, IF of three planes from a representative region of d41 SNO stained for sensory neurons (BRN3A (red) and NF (green)). No primary antibody control can be seen on the right. Scale bar, 20 μm .



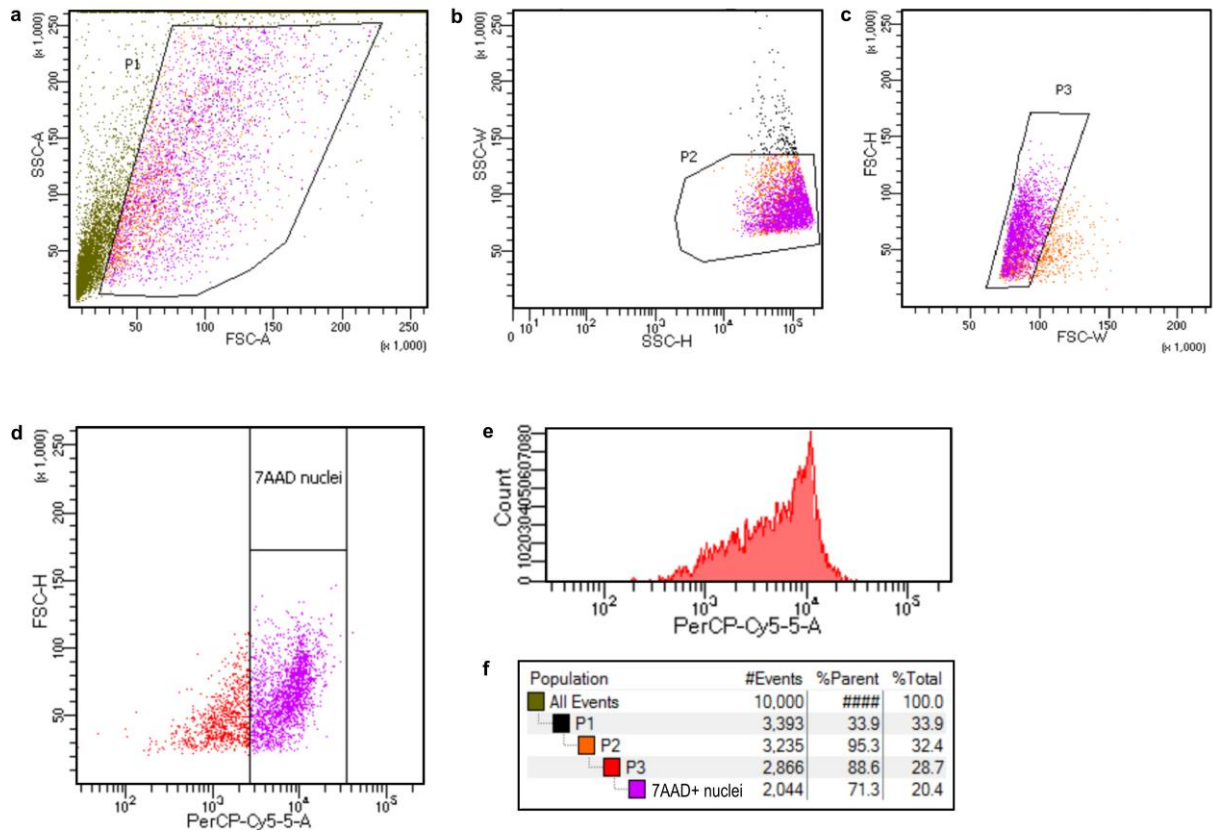
Supplementary Figure 4 | Neurotransmitter quantification by LC-MS/MS analysis. **a**, Representative LC-MS/MS spectra from lysed SNO and BENO for the noradrenaline, dopamine and acetylcholine compared to the respective standard at 1 μM concentration. **b**, Standard curves of all three neurotransmitters (concentrations from 1 μM to 0.001 μM). Linear regression (“through zero”) was calculated for the integrated peaks and used for quantification of the sample concentrations. Y-intercept and correlation coefficient r are indicated in the graphs.



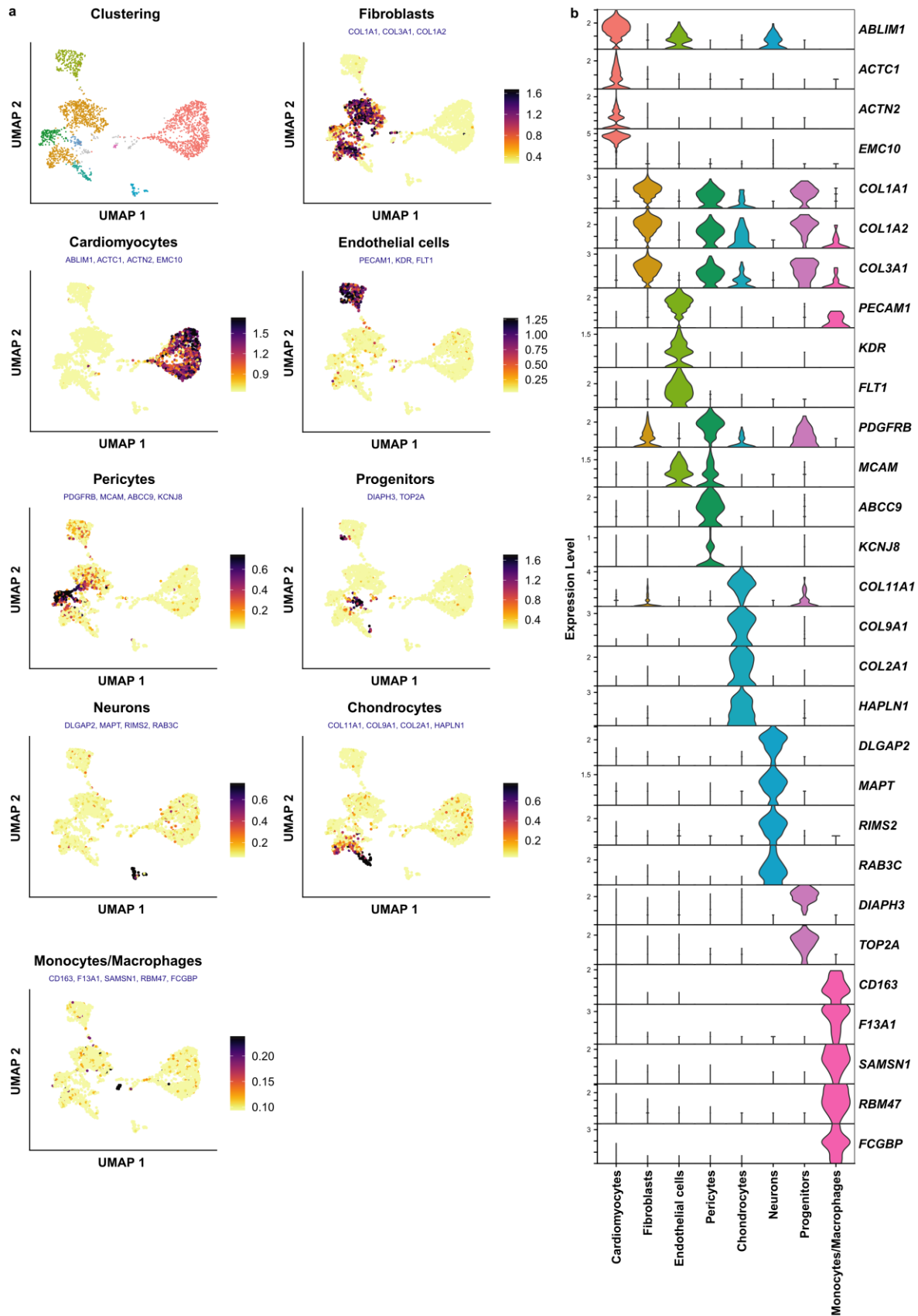
Supplementary Figure 5| Effect of nicotinic acid on electrical activity of SNO d73-87. a, Schematic of the placement of SNO on the multi-electrode array. **b,** Dose response curve of mean firing rate of SNO upon stimulation with escalating concentrations of nicotine normalized to basal firing rate and untreated control. $EC_{\text{Nicotine}50}=29.38 \mu\text{M}$, Nonlinear fit using variable slope (four parameters, ordinary fit). 3 independent differentiations, 6-7 biological replicates per differentiation ($n=19$), mean \pm s.e.m.



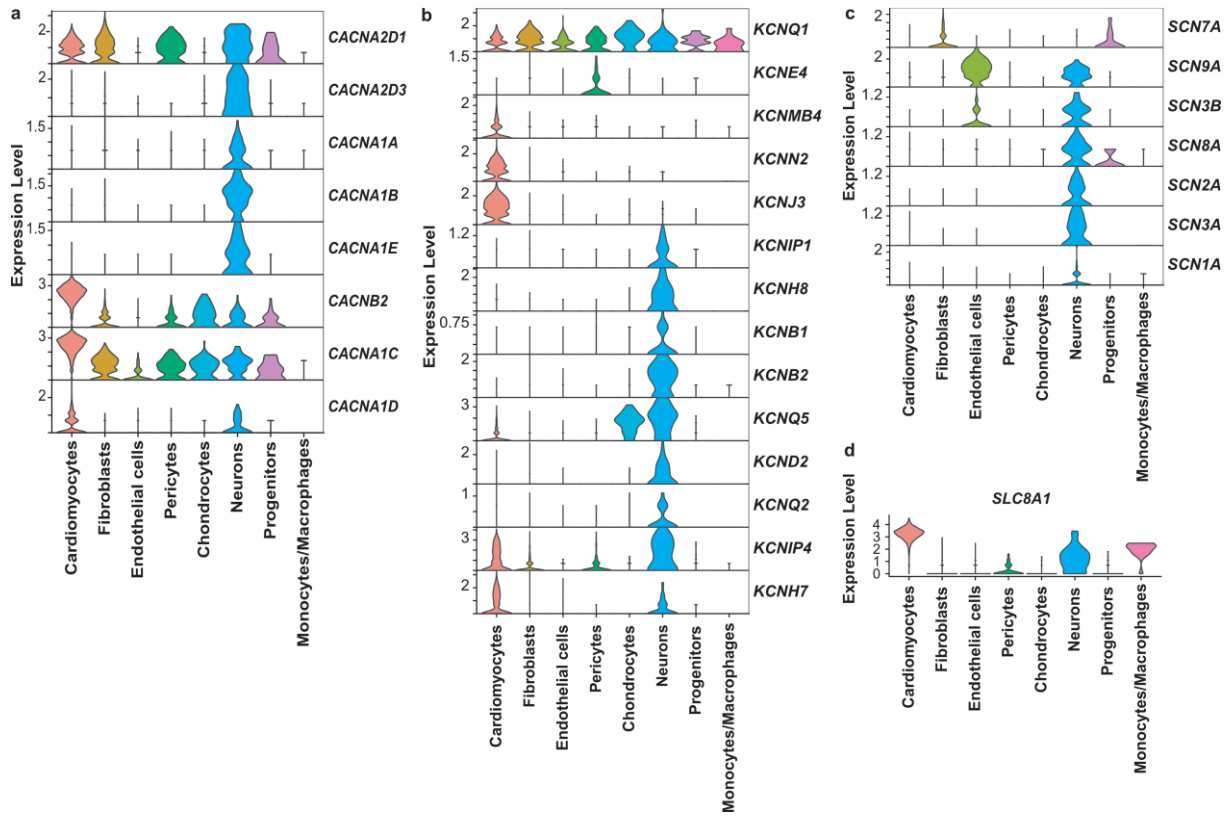
Supplementary Figure 6| Reproducibility of SNO differentiation protocol in three iPSC-lines. a, qPCR analysis of SN-marker DBH and TH, cholinergic marker SLC18A3 and CHAT as well as general neuron marker TUBB3 showed no difference between SNO from three different cell lines (RUCDRi002-A, BIHi001-A-2, UMGi093-A). Values were normalized to housekeeper and standard cell line RUCDRi002-A. **b,** WhIF of SNO from three different iPSC lines stained for DNA and SN-marker DBH and TH. Scale bar, 1 mm.



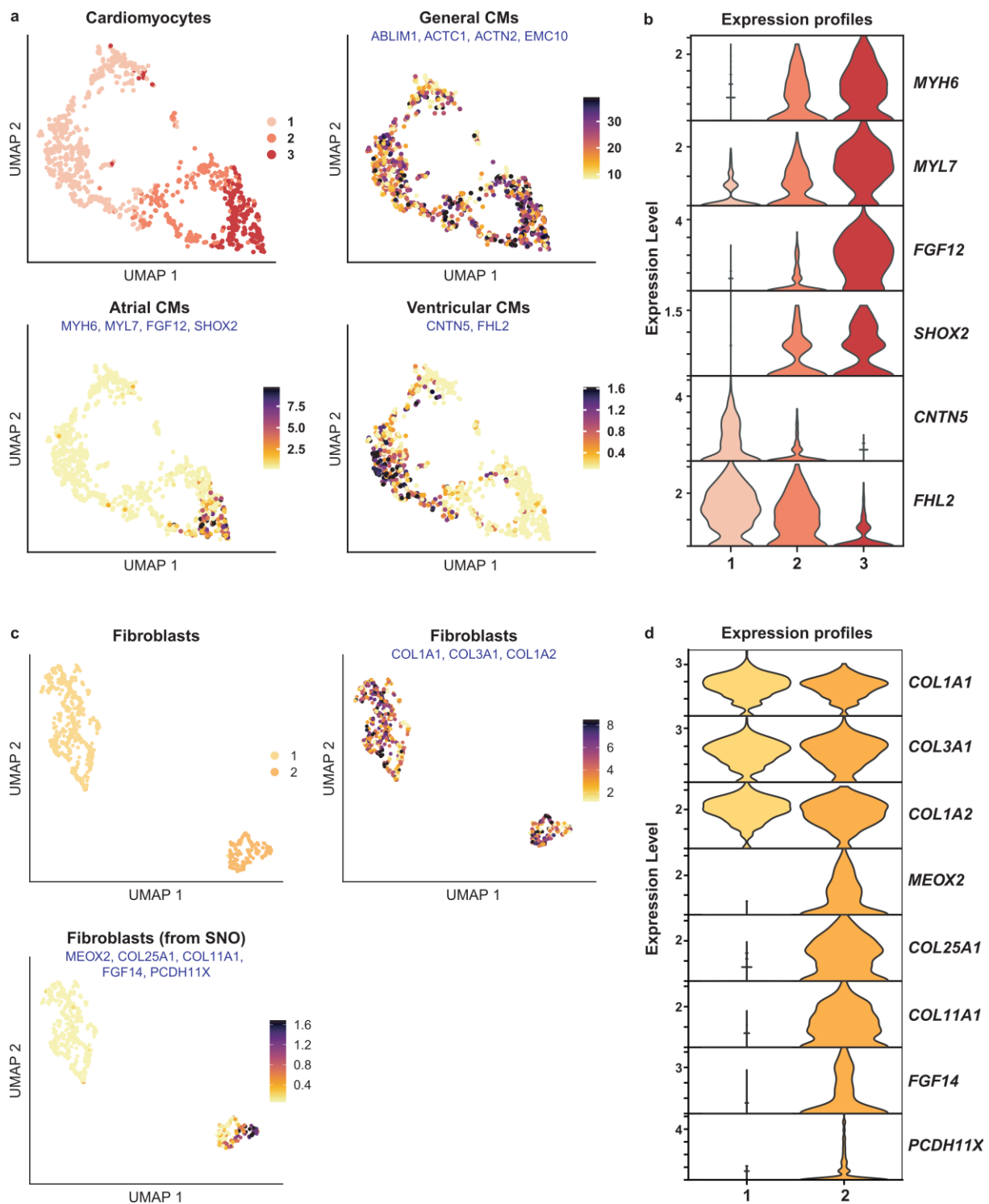
Supplementary Figure 7 | Gating strategy for sorting nuclei from frozen iEHM lysates using 7AAD staining. **a-c**, Gating strategy for exclusion of debris (P1, P2, P3) and for 7AAD-stained nuclei (**d**) from iEHM lysates. **e**, Hierarchy of the gated populations including proportions. **f**, Histogram of raw nuclei count (PerCP-Cy5.5 signal, 7AAD dye).



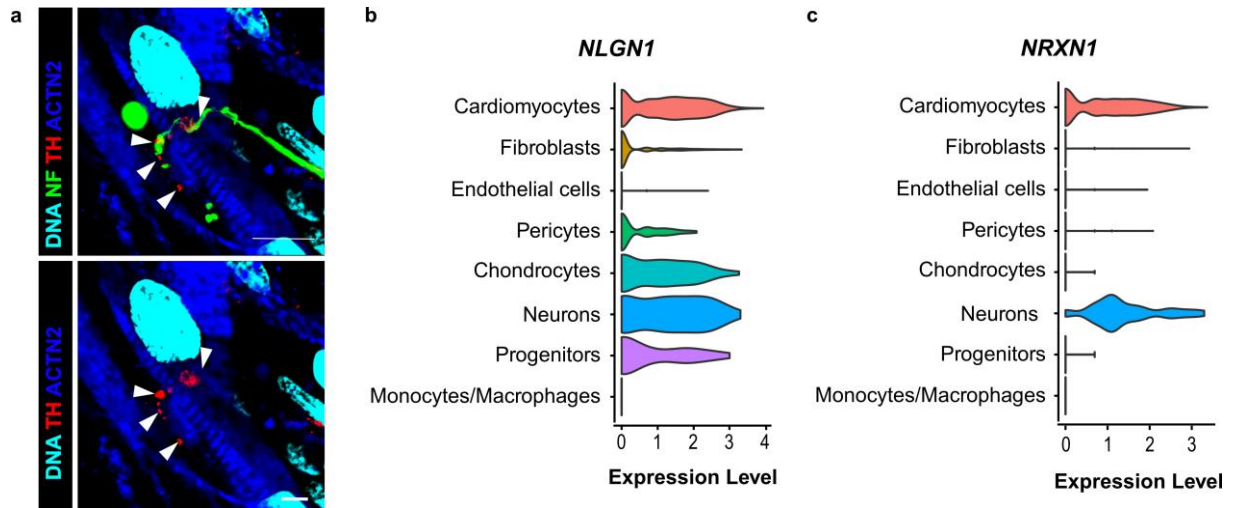
Supplementary Figure 8 | Cell cluster annotation of snRNA-sequencing. a, UMAP plots depicting the consensus expression (average module score) of cell-type specific marker genes used to annotate the clusters in the dataset. Gene names are highlighted in blue under the plot title of the corresponding cell-type. **b**, Violin plots showing the normalized expression of individual marker genes from **a** across the annotated cell-types.



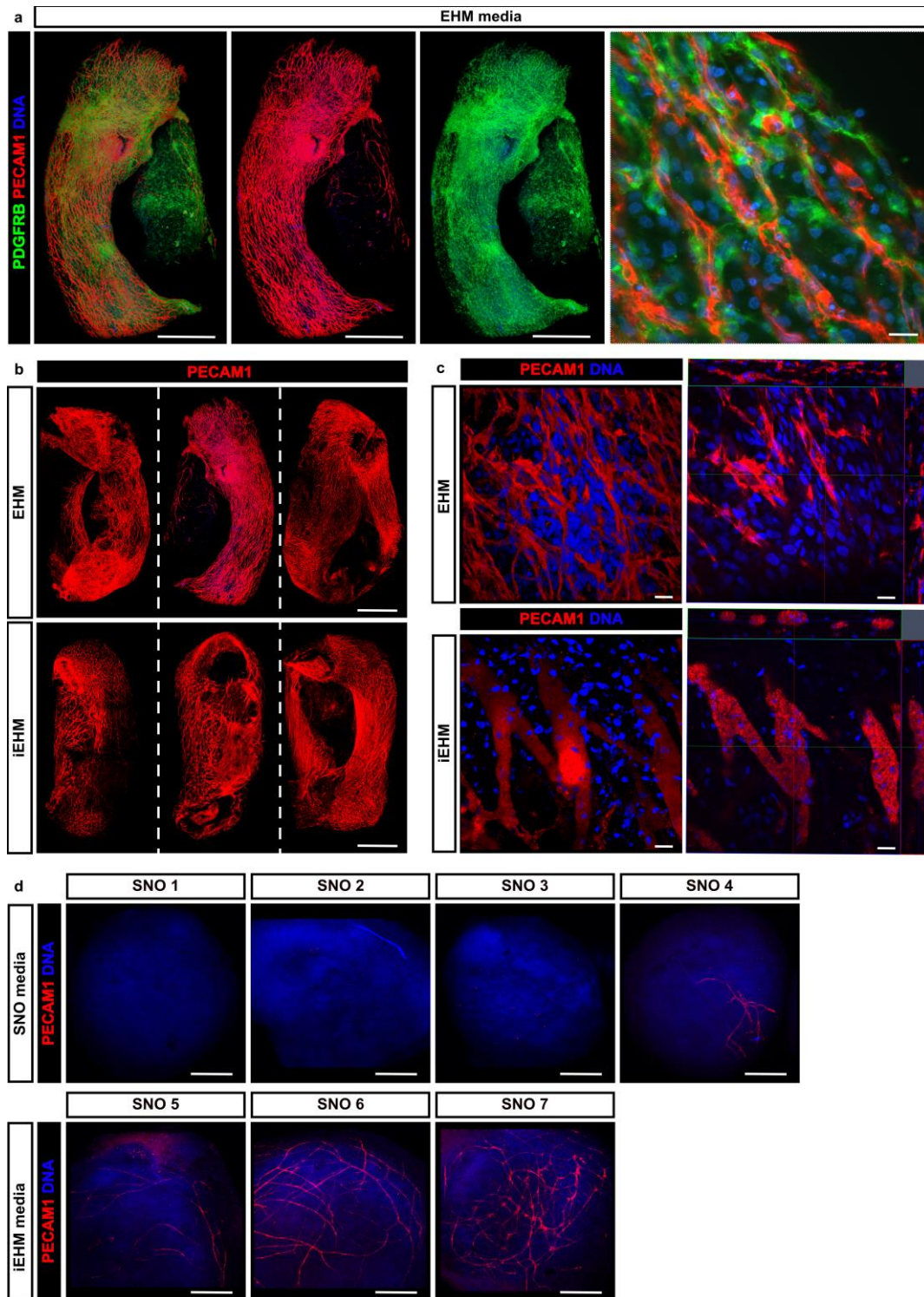
Supplementary Figure 9 | Expression analysis of ion channels across the cell types from snRNA-sequencing. Violin plots showing the normalized expression of **a**, voltage-gated calcium (Ca^{2+}) channel transcripts, **b**, voltage-gated potassium (K^+) channel transcripts, **c**, voltage-gated sodium (Na^+) channel transcripts and **d**, the $\text{Na}^+/\text{Ca}^{2+}$ exchanger *SLC8A1* transcript, across the annotated cell-types.



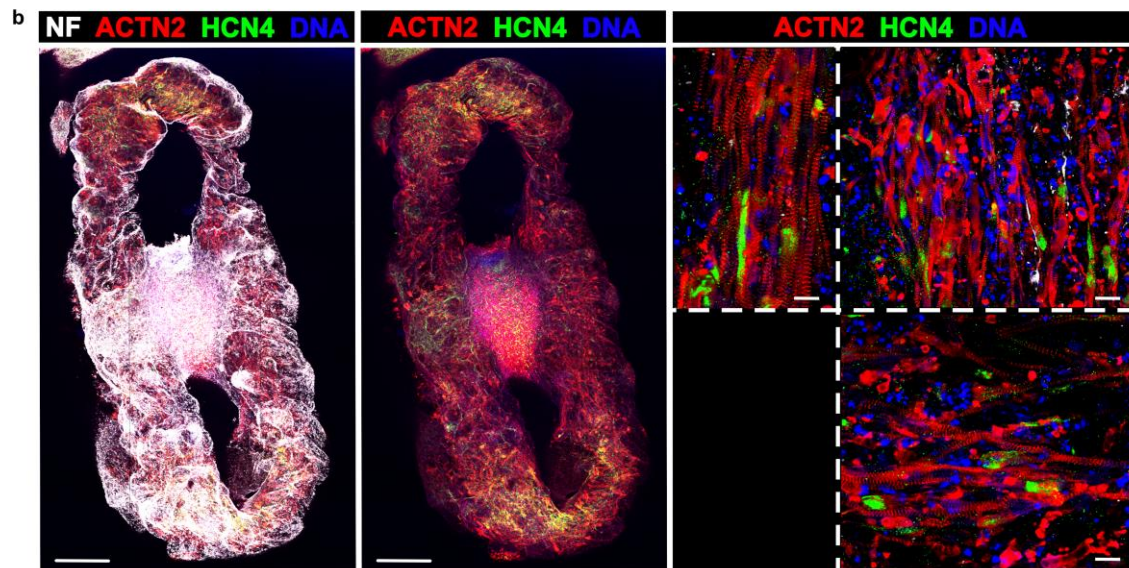
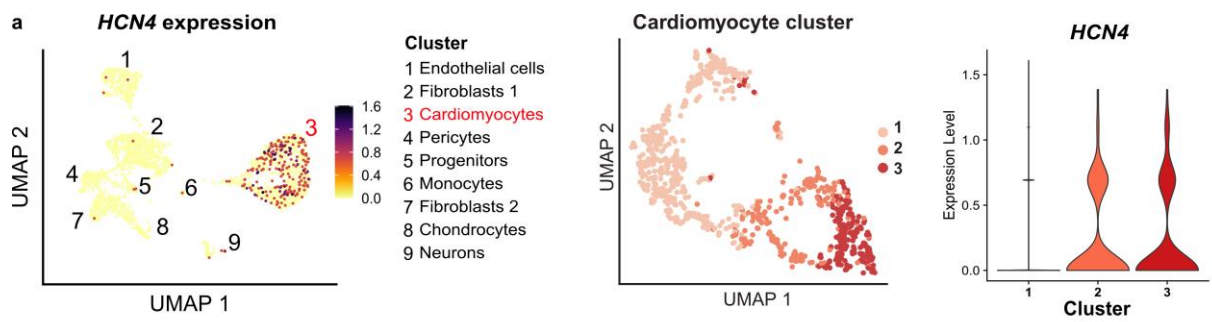
Supplementary Figure 10 | Analysis of cardiomyocyte and fibroblast subcluster in the iEHM. **a**, UMAP plots depicting the consensus expression (average module score) of atrial, ventricular and general cardiomyocyte marker genes across the cardiomyocyte sub-clusters (UMAP plot in the top-left panel). Gene names are highlighted in blue under the plot title of the corresponding sub-type. **b**, Violin plots showing the normalized expression of individual atrial and ventricular cardiomyocyte marker genes from **a** across the three sub-clusters. **c**, UMAP plots depicting the consensus expression (average module score) of fibroblast marker genes across the fibroblast sub-clusters (UMAP plot in the top-left panel). **d**, Violin plots showing the normalized expression of individual fibroblast marker genes from **c** across the two sub-clusters.



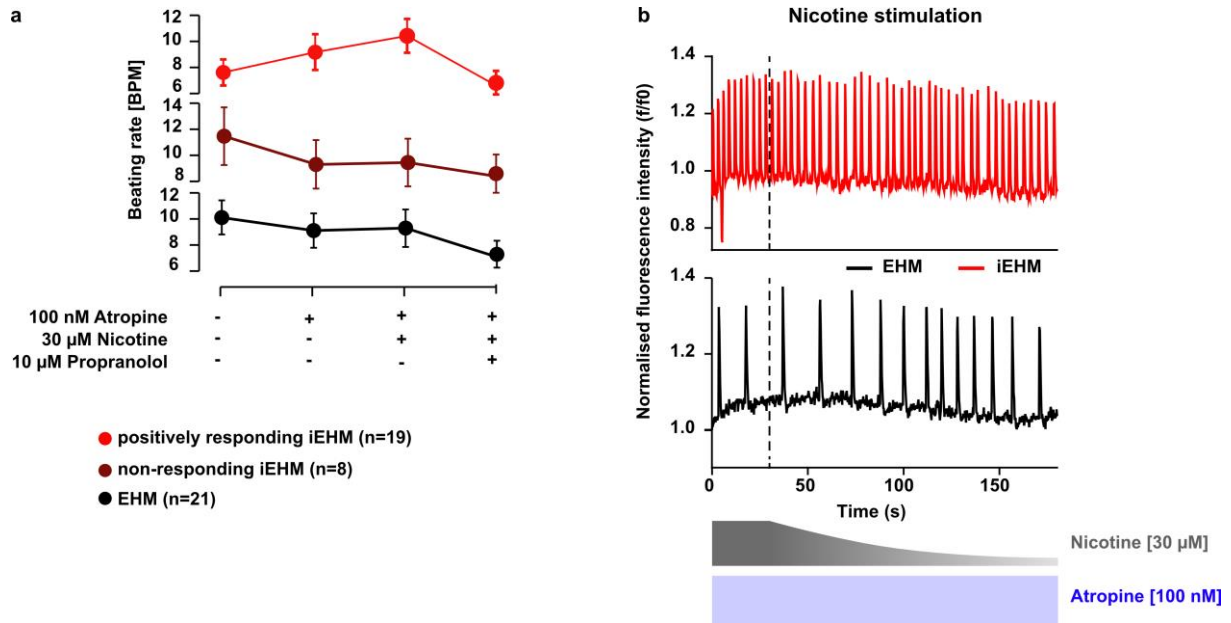
Supplementary Figure 11 | Investigation of neuro-cardiac junctions in iEHM. a, WhIF showing co-staining of synaptic bouton-like varicosity (NF, green) co-localizing with autonomic neuron marker TH (red) on the surface of cardiomyocytes (ACTN2, blue). Co-localization is indicated by white arrowheads. Scale bar, 10 μ m. **b**, Expression of postsynaptic adhesion molecule neuroligin 1 (NLGN1) across different cell types in the iEHM. **c**, snRNA sequencing expression analysis of presynaptic marker neurexin 1 (NRXN1) in the annotated iEHM cell clusters (see **Supplementary Figure 8**).



Supplementary Figure 12| Vascular network development in SNO, EHM and iEHM. **a**, WhIF of 6 weeks EHM cultured in EHM medium reveals a dense endothelial network (PECAM1, red) and presence of PDGFRb (green)-positive pericytes. Scale bar, 1 mm. **(Right)** Close-up view showing close localization of pericytes and endothelial cells. Scale bar, 20 μ m. **b**, PECAM1 (red) immunofluorescence analysis of three representative EHM and iEHM shows a similar extent of vascularisation of 6 week old EHM and iEHM. Scale bar, 1 mm. **c**, Close-up view of PECAM1 staining in EHM and iEHM **(left)** and the 3D-reconstruction **(right)** show a larger vessel diameter in some areas of the iEHM when compared to EHM. Scale bar, 20 μ m. **d**, **(Top)** WhIF of d93 SNO cultured exclusively in SNO media shows presence of endothelial cells in only one out of four tissues. **(Bottom)** After eight weeks of culture in iEHM medium, d103 SNO show the presence of endothelial cells in all of the screened tissues. Scale bar, 200 μ m.



Supplementary Figure 13| Identification of pacemaker-like cells in iEHM **a**, (Left) UMAP plots showing the distribution of cells expressing the pacemaker-like-cell marker HCN4 in the clusters in the dataset including cluster annotations (compare **Supplementary Figure 8**). (Right) Expression of HCN4 in the three cardiomyocyte cluster (Supplementary Figure 10). **b**, WhIF of iEHM stained for NF (grey), cardiomyocyte marker ACTN2 (red), pacemaker-like-cell marker HCN4 (green) and DNA (blue). (Left) Overview images show pacemaker-like-cells dispersed throughout the innervated areas of the EHM. Scale bar, 500 μ m. (Right) Close-up view show HCN4 positive cells in between ACTN2-positive CM co-localizing with NF-positive neurites (top left panel). Scale bar, 20 μ m.



Supplementary Figure 14| Details of pharmacological stimulation of iEHM. **a**, Chronotropic response to stimulation of EHM and iEHM with 100 nM atropine, 30 μ M nicotine and 10 μ M propranolol. iEHM could be separated into two distinct groups of responding ($N=19$) and non-responding tissues ($N=8$) that behaved similar to EHM controls. **b**, Example traces showing the acute effect of nicotine stimulation on EHM and iEHM mean fluorescence intensity (f/f_0) of the ROI (see in **Figure 3e**) in the presence of 100 nM atropine.

Supplementary Material

Supplementary Table 4. Detection parameters for a second compound-specific mass transition used as qualifier. Q1=first quadrupole, Q3=third quadrupole, DP=declustering potential, CE=collision energy, CXP=collision cell exit potential.

Compound	Mass Q1 [Da]	Mass Q3 [Da]	DP [V]	CE [V]	CXP [V]
Noradrenaline	170.2	152.0 (107.0)	36	10 -28	10 -20
Dopamine	154.1	137.2 (91.0)	36	15 -33	10 -8
Acetylcholine	147.0	87.0 (88.0)	36	19 -20	16 -16
Noradrenaline-d6	176.1	158.0 (111.0)	31	11 -29	10 -6
Buformin	157.91	60.9 (47.0)	36	35 -66	10 -8
Choline-d9	113.108	69.1 (66.1)	66	27 -44	12 -12

Supplementary Table 5. List of primer for quantitative real-time PCR.

Gene	Forward primer	Reverse primer	Amplicon length (bp)
ASCL1	CGGTCTCATCCTACTCGTCCG	GTTGTGCGATCACCTTGCTT	150
CHAT	GGATCGCTGGACATGATTG	CCACACCGCCAGGTCCG	103
DBH	TGGGTGCCAAGGCATTTTAC	ATGCCTGAGGAGTCGTTTCG	136
GAD1	AGGCAATCCTCCAAGAACC	TGAAAGTCCAGCACCTTGG	218
GAPDH	CCTCAAGATCATCAGCAATGCC	ATGTTCTGGAGAGCCCCGC	189
GATA2	GCAGAACCGACCACTCATCA	AGTGGCCTGTTAACATTGTGC	177
GBX2	GTTCCCGCCGTCGCTGATGAT	GCCGGTGTAGACGAAATGGCCG	118
GLAST	CCCCTTACAAAATCAGAAAAGTTGT	CCCATCTTGGGCTCTTCTCC	151
MNX1	TGCCTAAGATGCCGACTTC	AATCTTACCTGGGTCTCGG	194
OLIG2	GCTGCGTCTCAAGATC	AGTCGCTTCATCTCCT	192
PAX6	CCCCACATATGCAGACACAC	TCACTCCGGAACCTTGAAC	112
PHOX2B	CGCCGCAGTTCCCTTACAAAC	TGTCGGGGTAGTGAGTCTCC	140
PRPH	TAAATATAAAGACGACTGTGCCTGA	GCAGAAGACTTGTCCAGCTCA	151
SLC17A6	GTAGACTGGCAACCACCTCC	CCATTCAAAGCTTCCGTAGAC	129
SLC18A2	TTCCGACTGTCCCAGTGAAG	TGCTGGAGAAGGCAAACATAAT	200
SLC6A2	CAGGTTCCAGCAACGACATCCAG	GTCGTAGGTGAGTGGCTTGAAG	142
TH	CGGGGCTTCTCGGACCAGGTGTA	CTCCTCGGCGGTGTACTCCACA	111
TUBB3	CAGCGTCTACTACAACGAGG	AGGCCTGAAGAGATGTCCAA	121
SLC18A3	CTGCTAGTGAACCCCTTGAGC	CAGGACTGTAGAGGCGAACAT	99

Supplementary Table 6. List of primary and secondary antibodies.

Antigen	Modification	Brand	Cat. No.	Host	Dilution	Type
ACTN2	None	Sigma	A7811	Mouse	1:1000	Primary
BRN3A	None	Merck Millipore	MAB1585	Mouse	1:500	Primary
CTNT	None	Abcam	ab45932	Rabbit	1:250	Primary
DBH	None	Sigma	HPA070789	Rabbit	1:100	Primary
HCN4	None	Abcam	ab69054	Rabbit	1:200	Primary
Neurexin 1	None	Sigma	HPA071400	Rabbit	1:200	Primary
NF (H)	None	Synaptic Systems	171 106	Chicken	1:100	Primary
NF (H)	None	Biologend	822601	Chicken	1:1000	Primary
PAX6	None	Biologend	901301	Mouse	1:500	Primary
PDGFRb	None	Cell Signalling	28E1	Rabbit	1:100	Primary
PECAM1	None	DAKO	M0823	Mouse	1:100	Primary
Peripherin	None	NOVUS	NBP1-05423	Chicken	1:1000	Primary
Phalloidin	Alexa Fluor 488	Invitrogen	A12379	-	1:200	Coupled
PHOX2B	None	Santa Cruz	sc-376997	Mouse	1:250	Primary
Synapsin 1	None	Synaptic systems	106 011	Mouse	1:200	Primary
TH	None	Synaptic Systems	213 004	Guinea pig	1:500	Primary
vAChT	None	Synaptic Systems	139 103	Rabbit	1:500	Primary
VGLUT1	Abberior STAR 635P	NanoTag	N1602-Abb635P	Rabbit	1:250	Coupled
Mouse	Alexa Fluor 633	Invitrogen	A21052	Goat	1:400	Secondary
Chicken	Alexa Fluor 488	Invitrogen	A11039	Goat	1:400	Secondary
Rabbit	Alexa Fluor 546	Invitrogen	A11035	Goat	1:400	Secondary
Guinea Pig	Alexa Fluor 546	Invitrogen	A11074	Goat	1:400	Secondary

Supplementary Videos

Supplementary Video 1. Spontaneous beating of iEHM 1 week after fusion

Supplementary Video 2. Representative immunofluorescence picture depicting neurofilament positive axons (green) interlacing alpha-actinin positive cardiomyocytes (red) in iEHM

Supplementary Video 3. Representative immunofluorescence picture 1 depicting synapsin positive pre-synaptic terminals (red) of noradrenergic neurons (TH, blue) in between cardiomyocytes (cTNT, green) in 8 week-old iEHM.

Supplementary Video 4. Representative immunofluorescence picture 2 depicting synapsin positive pre-synaptic terminals (red) of noradrenergic neurons (TH, blue) in between cardiomyocytes (cTNT, green)) in 8 week-old iEHM.

Supplementary Video 5. Representative immunofluorescence picture 3 depicting synapsin positive pre-synaptic terminals (red) of noradrenergic neurons (TH, blue) in between cardiomyocytes (cTNT, green)) in 8 week-old iEHM.

Supplementary Video 6. Representative immunofluorescence picture 4 depicting synapsin positive pre-synaptic terminals (red) of noradrenergic neurons (TH, blue) in between cardiomyocytes (cTNT, green)) in 8 week-old iEHM.

Supplementary Video 7. Representative immunofluorescence picture 5 depicting synapsin positive pre-synaptic terminals (red) of noradrenergic neurons (TH, blue) in between cardiomyocytes (cTNT, green) in 8 week-old iEHM.

Supplementary Video 8. Representative immunofluorescence picture 6 depicting synapsin positive pre-synaptic terminals (red) of noradrenergic neurons (TH, blue) in between cardiomyocytes (cTNT, green) in 8 week-old iEHM.

Supplementary Video 9. Representative immunofluorescence picture 1 depicting PECAM1 positive vascular network (red) surrounded by PDGFRb positive pericytes (cyan) in close proximity to neurons (NF, green) in 8 week-old iEHM.

Supplementary Video 10. Representative immunofluorescence picture 2 depicting PECAM1 positive vascular network (red) surrounded by PDGFRb positive pericytes (cyan) in close proximity to neurons (NF, green) in 8 week-old iEHM.

Supplementary Video 11. Representative immunofluorescence picture 3 depicting PECAM1 positive vascular network (red) surrounded by PDGFRb positive pericytes (cyan) in close proximity to neurons (NF, green) in 8 week-old iEHM.

Supplementary Video 12. Chronotropic response of EHM and optogenetic iEHM evoked by light stimulation